Available online at http://www.ijprt.org.tw/

Chinese Society of Pavement Engineering

International Journal of Pavement Research and Technology 11 (2018) 747-758

http://www.ijprt.org.tw/

Case study of longitudinal thermal cracking related to asphalt concrete pavement construction

Martin Lavoie [a,*], Félix Doucet [b], Maxime Laplante-Boivin [b]

[a] Ministère des Transports, de la Mobilité durable et de l'Électrification des Transports, 880 chemin Ste-Foy, Quebec City G1S 2L2, Canada
[b] Ministère des Transports, de la Mobilité durable et de l'Électrification des Transports, 2700 rue Einstein, Quebec City G1P 3W8, Canada

Received 2 November 2017; received in revised form 14 February 2018; accepted 28 March 2018

Keywords: Cracking; Thermal imaging; Segregation; Thermal streaks; CT-scan; Asphalt mix

1. Introduction

Every year, the Ministère des Transports, de la Mobilité Durable et de l'Électrification des Transports (MTMDET) provides for the laying of several million tonnes of asphalt to ensure the maintenance and development of the Quebec road network. Observations on roads over the past few decades have shown that the premature occurrence of certain types of surface defects after asphalt paving occurred on a regular basis. After a study conducted in 2005, infrared imaging technology has made it possible to establish links between these defects and the thermal signature of an asphalt mat before compaction [1].

This technology has been implemented gradually as a mean to control the quality of asphalt paving. Technical clauses and a measuring procedure on construction sites have been included in many MTMDET contracts since 2008.

Monitoring of different sites and special expert studies conducted over the past few years have allowed further demonstration of the effects of heterogeneous temperature in the asphalt mix, particularly thermal streaks, on pavement behavior. These studies were based on thermal imaging and mechanical properties' analyses to better understand the longitudinal thermal cracking phenomenon.

2. Literature review

Longitudinal cracking is a commonly observed degradation on asphalt pavements. This asphalt layer defect, which develops parallel to the direction of the road, is often associated with fatigue or structural deficiency when it is in the wheel paths. When it is outside of the wheel paths, the most recognized causes are the effect of frost, differential settlement, failure of a longitudinal construction joint or segregation in the mix [2,3]. Fig. 1 shows longitudinal cracking observed on the Quebec road network, associated with construction defects in these cases.

For over a decade, several researchers have been focusing on this type of cracking by associating it with a down-cracking phenomenon called "top-down cracking." Explanations as to the source of the phenomenon are varied. According to some [4], the development of longitudinal top-down cracking is associated with the distribution of stresses due to tire loads typically located near the wheel paths. Initiation of the crack from the surface seems to depend on surface tension stresses. However, this theory does not entirely explain cracks that develop outside of wheel paths as regularly seen on roads [1,5]. There are many explanations for the crack development mechanism [6]. We find a large number of factors contributing to the phenomenon of top-down cracking; low tensile strength

* Corresponding author.
E-mail addresses: Martin.Lavoie@transports.gouv.qc.ca (M. Lavoie), Felix.Doucet@transports.gouv.qc.ca (F. Doucet), Boivin@transports.gouv.qc.ca (M. Laplante-Boivin).
Peer review under responsibility of Chinese Society of Pavement Engineering.

https://doi.org/10.1016/j.ijprt.2018.03.006
1996-6814

Fig. 1. Examples of longitudinal cracking associated to asphalt segregation.

of the mix, segregation, rigidity difference, thermal contraction and expansion, bitumen aging, etc.

Several authors have identified asphalt segregation as the cause to explain the top-down cracking phenomenon [4–9]. Their publications focus on the study of a crack creation mechanism by tensile and thermal stresses. Some are more explicit and directly target the problem associated with pavers, one that concerns MTMDET the most [10–12]. Colorado DOT studies have helped establish clear links between the location of cracks and preferential segregation axis on a paver. These researchers [10,12] agree that segregation is not easily visually detectable and that it is not possible to quantify particle size differences from analyses of core samples because segregation is confined in a limited area.

The preferential axes in which the flow of the mix may not be regular, explained in a document from a paver manufacturer are shown in Fig. 2 [13].

Depending on the type of paver, the location of these preferential axes are either in the center of the equipment under the gearbox of the auger, the outer limits of the conveyors, the edge of the fender, the auger bearing hanger, or the end gate. The distribution of the mix in the screed of the paver and from non-uniform mix feeding. It is recognized in the literature that this presence of segregation streaks is associated with a malfunction of the paver or its operation mode [13].

The State of Illinois conducted a study [4] on the top-down cracking phenomenon which explains its link to the existence of a thin plane of weakness created by pavers, in which a crack can be initiated. This possibility has already been mentioned in some manuals on distress identification including the Ministry of Transportation of Ontario [3].

Moreover, a study from Indiana [9] concludes that infrared imaging would be an excellent method to detect segregation and identify asphalt laying problems. Thermal streaks found in studies using this tool have confirmed that the relationship between longitudinal cracking and paving practices is realistic [1,14]

3. Thermal streaks detection with thermal imaging

3.1. Thermal streaks

Fig. 3 shows two examples of thermal streaks observed immediately behind the paver during laying of the mix. The location of the streaks corresponds to some of the

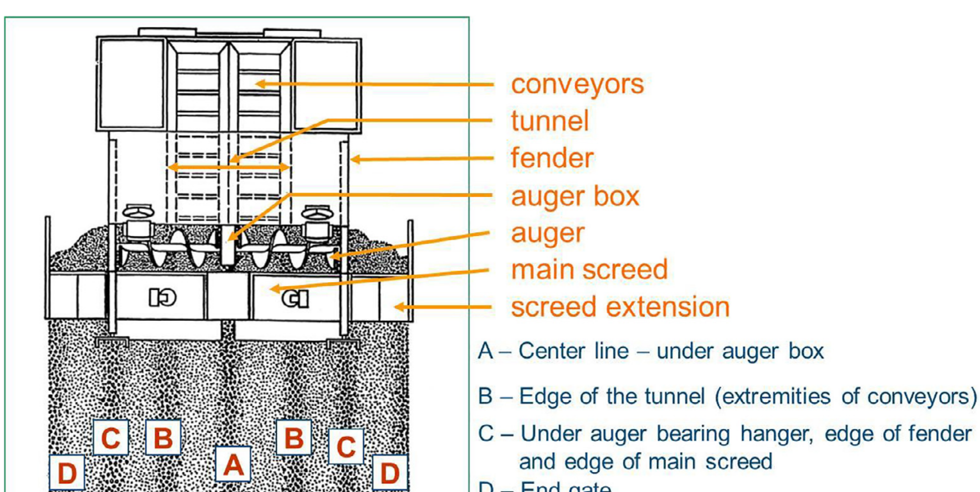

Fig. 2. Preferential segregation axes (adapted from [13]).

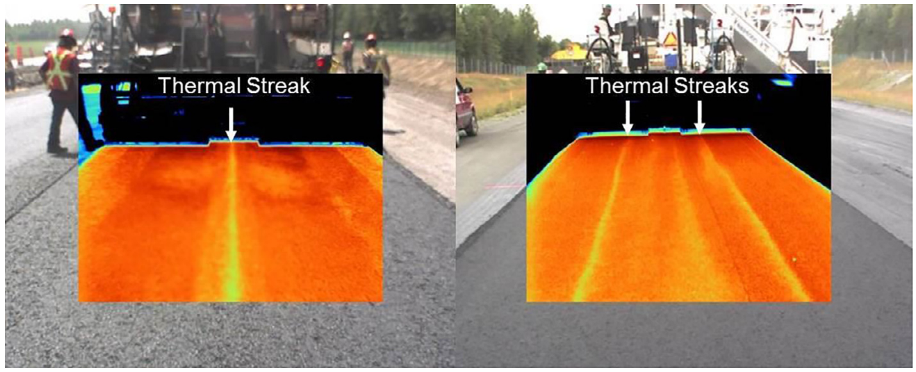

Fig. 3. Examples of thermal streaks at different locations on the mat detectable with thermal imaging.

preferential axes shown in Fig. 2 (left side: center of paver; right side: edges of conveyors). Differences in temperature and differential cooling in the mat on a specific axis is caused by a lower density of asphalt or a discontinuity that allows a greater loss of heat. The phenomena can be created in front or under the paver screed and results in a difference in temperature just behind the screed. These differences of temperature can be as low as 5 °C.

3.2. Automated thermography system

MTMDET have developed an Automated Thermography System (ATS) that operates throughout the asphalt laying process. The system has been used by some contractors in recent years. It was developed in order to offer contractors a better monitoring tool to view the thermal effect of operations and paver adjustments in real-time, and to facilitate auto-control. Automation proved to be an excellent way to help control the equipment thereby avoiding the thermal streaks phenomena [15]. The last AASHTO specification PP 80-14 “Standard Practice for Continuous Thermal Profile of Asphalt Mixture Construction” involving tools like temperature sensor bar (IR-Bar) or infrared scanner (IR-Scanner) is currently implemented and will focus, among others, on thermal streaks phenomena [16].

4. Case study

4.1. Investigations

Over the past few years, the MTMDET has made significant investments toward its road network. The majority of new hot mix asphalt layers have been monitored by thermography to evaluate the homogeneity during placement.

After several years in service, some of the road segments have presented defects and premature cracking. Studies were conducted in some cases where longitudinal cracking appeared just few months after construction to find out if it could be the result of segregation and linked to thermal streaks detected during construction. In order to determine the cause of damage and to characterize segregation in the mix, an investigation involving coring in different sectors, analyses of the mix physical characteristics, mechanical tests on samples and analyses using tomodensitometry was performed. The roads of the cases studied are located in the eastern part of the province of Quebec in Canada (GPS Coordinates: 47°33′ N, 68°41′ W).

Fig. 4 shows (a) a thermal image with two axes showing thermal streaks detected during the laying of the bituminous layer, (b) longitudinal cracking present in the pavement in segregated axis, (c) a sampling sector with cores in the axis of segregation and cores outside the axis, and also (d) cores from the axis of segregation and outside the axis.

Sectors comprising a set of cores in the axis of segregation and an additional set for another parallel axis toward the center of the lane were probed for comparison purposes. The cores in the segregation axis were not probed directly from the cracked zone in order to be able to perform tests on non-dislocated samples and obtain reliable results. Other cores near the sectors were taken occasionally directly to the location of the longitudinal cracking specifically for the observation of the phenomenon.

The comparative observation of cores from various sectors revealed that the arrangement of the aggregates in the top layer is generally different in the axis of segregation since there are more voids and coarser aggregates. The cores taken outside the axis of segregation (0.6 m distance toward the center of the lane) has a generally more uniform appearance.

4.2. Conventional characteristics

Cores from nine different sectors were analyzed to determine their physical characteristics (particle size, bitumen percentage, and air void content). The particle size distributions of the two different sets of cores (segregation axis and off-axis) are presented in Fig. 5. The curves of the segregation axis are generally under the job mix formula curve, on the coarser side, while those of the off-axis are close to the targeted formula.

Fig. 6 shows all results for the GB-20R-type mix based on the main reference sieves that help better discriminate the content of coarse aggregates (5 and 10 mm). The over-

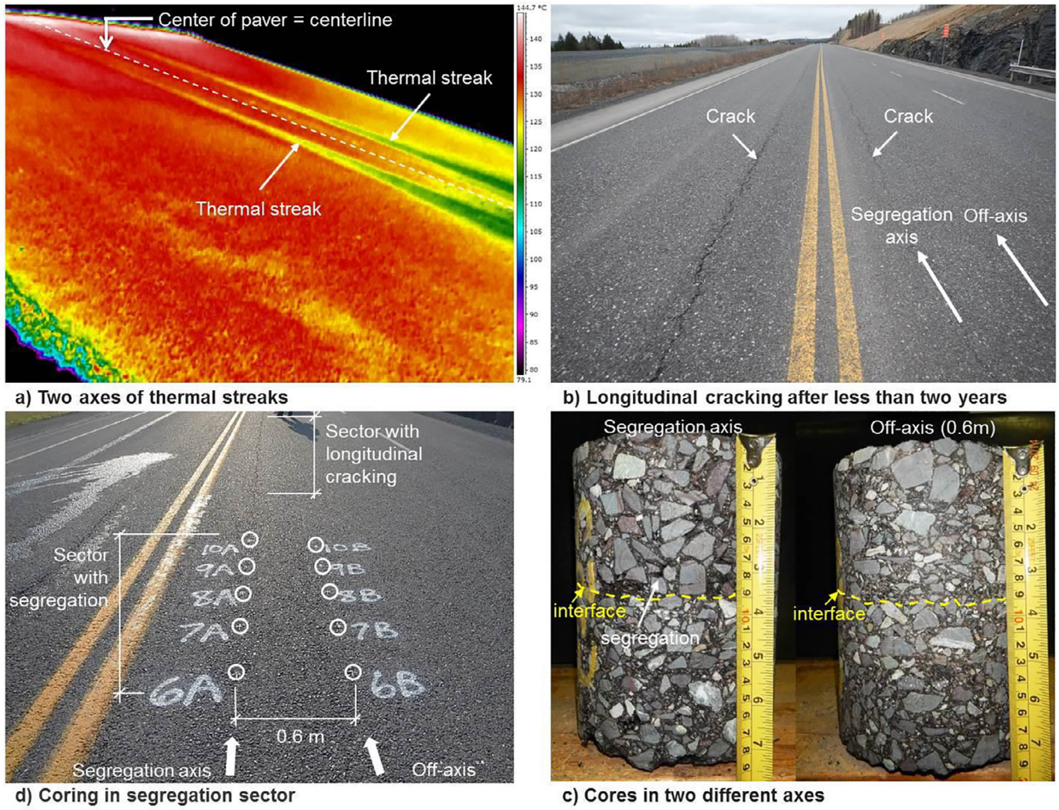

Fig. 4. Case study with comparison cores.

all average and the standard deviation limits are shown in the last column of the two graphs. For both sieves, the overall average of percentage passing was about 6% lower (significantly different statistically based on comparison of sums of mean and standard deviation as well as possible overlap of values) in the axis of segregation, which means that the asphalt mix in this axis is composed of a greater amount of coarse aggregates.

Also, the layer affected by segregation has, on average, 0.3–0.4% less bitumen and 1–2 % more air voids compared to the "off-axis" asphalt. The overall results of these series of cores denote differences in the composition of the mix in the problematic axis. These differences in properties are significant compared to the rest of the asphalt mat.

4.3. Mechanical properties

Complex modulus (E^*), creep compliance ($D(t)$) and tensile strength (S_t) tests were carried out on cores from seven sectors where thermal streaks were observed in order to assess thermal cracking resistance of the asphalt mix. These tests were preceded by bulk density and water absorption tests to evaluate the impact of physical characteristics on the mechanical properties of the asphalt mix.

Three cores were sampled at 1 m intervals for each sector and have subsequently been cored again to get specimens of 75 mm diameter by 130 mm high according to the LC 26-690 test method [17]. The specimens were cored horizontally and transversely to the direction of traffic to study the transverse thermal shrinkage of the mix, as shown in Fig. 7. Only the layer in surface was characterized in this study.

Table 1 summarizes tests results obtained for the seven sectors investigated regarding four different parameters for the two compared axes (air void content, water absorption, dynamic modulus and tensile strength). The average results and the standard deviations for the three specimens of each sector are shown by position (axis of segregation versus off-axis). It is also specified if the results between the two axes are significantly different statistically or not, based on comparison of sums of mean and standard deviation as well as possible overlap of values.

Air void content and water absorption of the specimens were determined according to the LC 26-040 [18] and LC 21-067 [19] test methods, respectively. The air void content of the specimens located in the segregation axis is higher than those "off-axis". The difference can be up to 1.7% (on average 0.8%) between the air void content of the two axes. The water absorption values in the segregation axis are two to nine times greater (on average three times), indicating a significantly higher porosity of the specimens in the segregation axis associated with a concentration of air voids.

The complex modulus (E^*) of the specimens was determined according to the LC 26-700 test method [20] since it is a non-destructive test commonly used by the

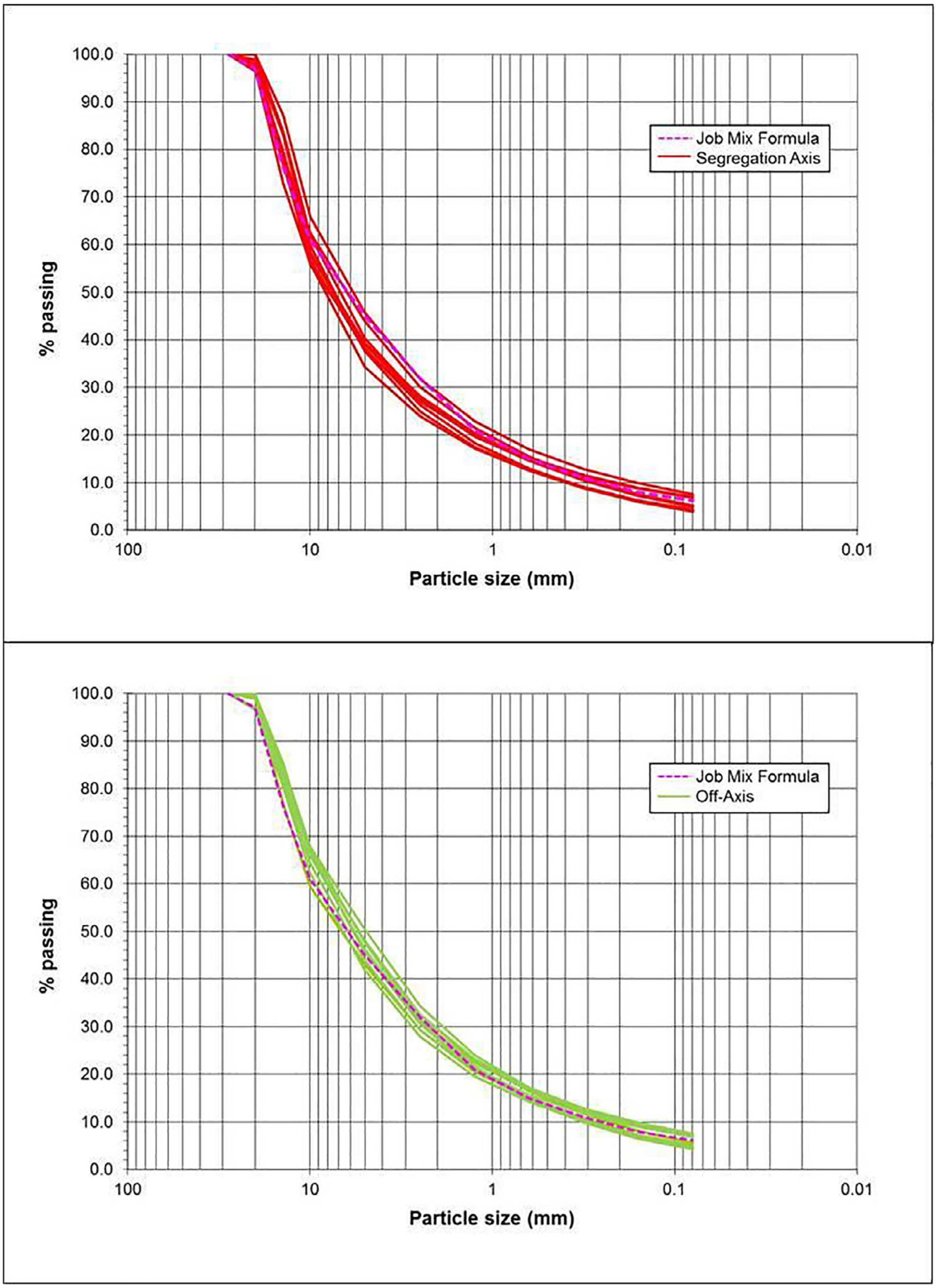

Fig. 5. Particle size distribution for segregation axis cores (top) and off-axis cores (bottom).

MTMDET to assess the mechanical behavior of asphalt mix [21,22]. The tests were carried out only at the intermediate temperature of 10 °C used as a reference by the MTMDET to determine the master curve of E^* [23], in order to limit the number of tests to be performed.

Table 1 shows the mean results of dynamic modulus ($|E^*|$) of the three asphalt mix specimens by position for the different sectors at 10 °C and 10 Hz, which represent the intermediate testing conditions of the asphalt mix on highways in Quebec [24]. The $|E^*|$ is the intensity of the E^* defined by Eq (1).

$$|E*| = \frac{\sigma}{\varepsilon} \quad (1)$$

where
$|E^*|$ is the dynamic modulus (MPa);
σ is the stress (MPa); and
ε is the strain (m/m).

The mean $|E^*|$ of the asphalt mix in the segregation axis is significantly lower in all studied sectors, except for sectors 1 and 4 where the gap is smaller. The differences of $|E^*|$ vary from 4 to 44% between the axes for all sectors.

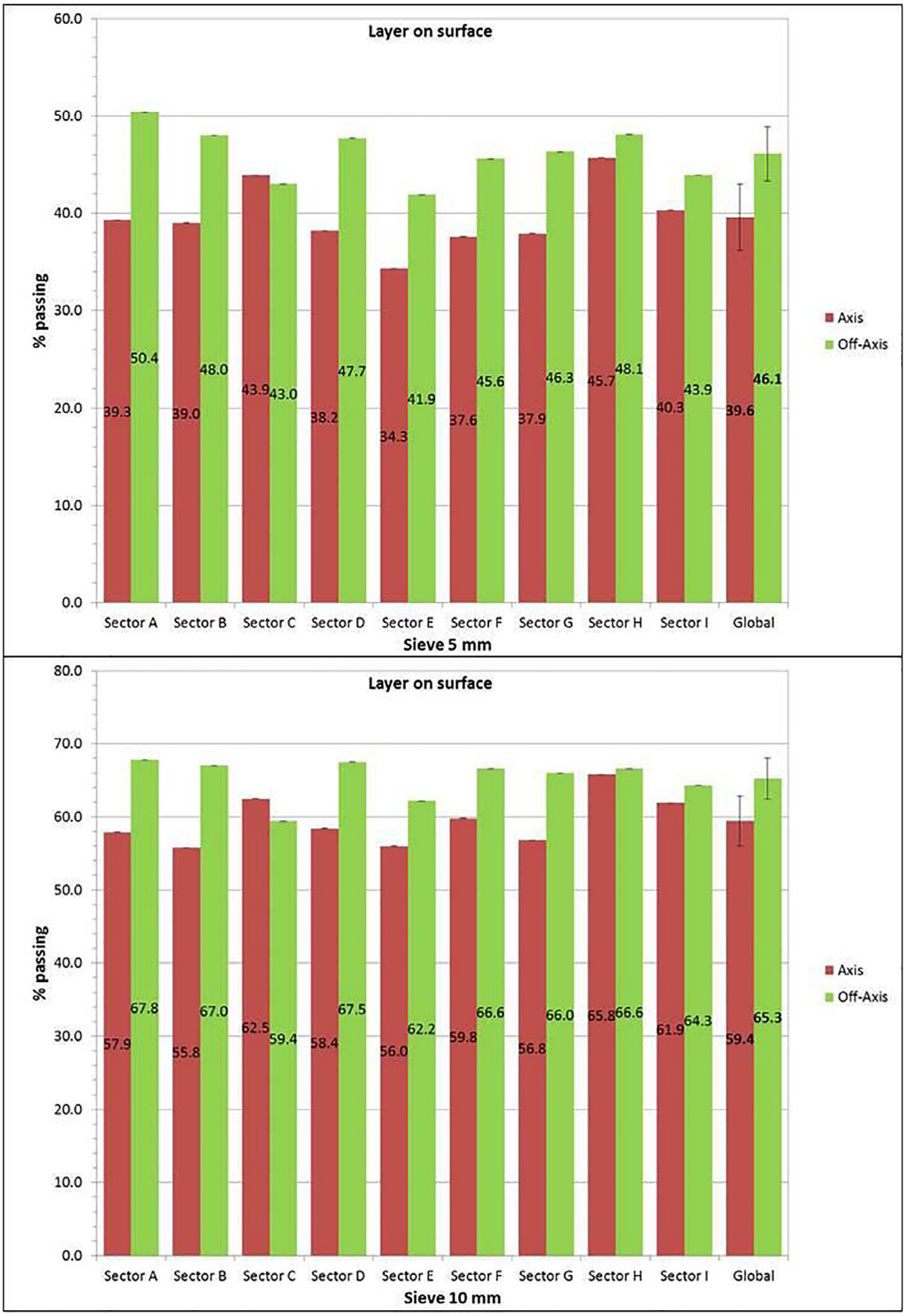

Fig. 6. Granular comparison for the 5 mm (top) and 10 mm (bottom) sieves on cores for the surface layer.

Fig. 8 shows that there is a relationship between the $|E^*|$ and the water absorption results ($R^2 = 0.44$). The $|E^*|$ varies from about 7800 MPa for 0.1% absorption to 5600 MPa for 1.0% absorption, which is a significant difference of $|E^*|$. The water absorption variations can therefore indicate significant differences in dynamic modulus between the segregation axis and the rest of the lane, which may cause differences in the general mechanical behavior of the mix.

The creep compliance ($D(t)$) of the asphalt mix was then determined according to AASHTO T322 test method. This is a non-destructive test used by AASHTOWare Pavement ME Design to predict thermal cracking of asphalt mix. The average results obtained only show minimal differences between the samples in the segregation axis and off the axis, indicating that segregation does not appear to affect the creep compliance of asphalt mix.

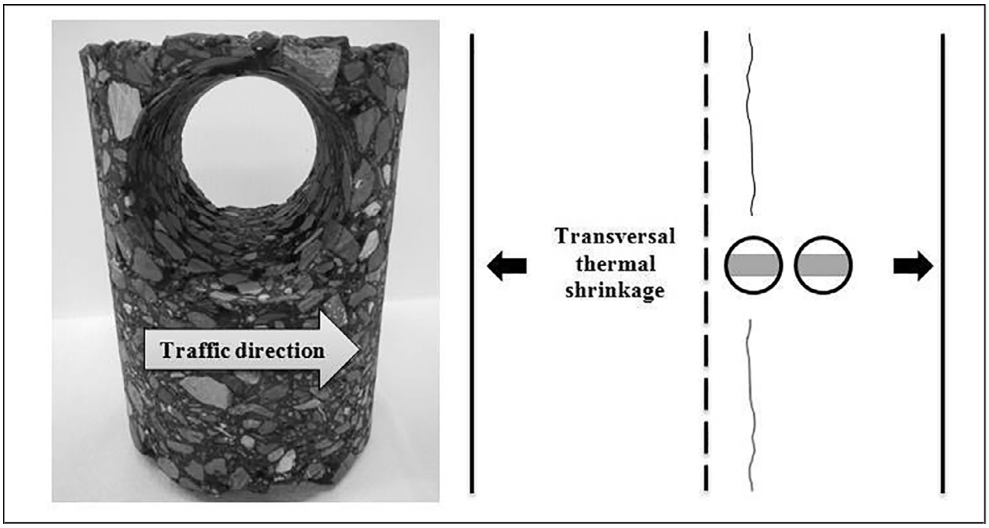

Fig. 7. Coring of specimen in the surface layer.

The tensile strength (S_t) of asphalt mix was determined according to the AASHTO T322 method. This is a tensile failure test used by Pavement ME to predict asphalt mix thermal cracking. The tests were performed under direct traction at −10 °C following the E^* tests. The St was determined at a tensile strain rate of 240 με/s.

The mean S_t at −10 °C of the surface mix according to the position and the sector are shown in Table 1. The S_t is significantly lower in the segregation axis for all cases, which means that the asphalt is less resistant to thermal stress in this axis. The tensile strength differences between the axes vary between 15% and 46% for the sectors studied.

Fig. 9 shows good relationship between the S_t and water absorption ($R^2 = 0.77$) which indicates that the S_t decreases as porosity increases. Larger water absorption indicates a concentration of air voids in some places, which implies that the tensile force is distributed over a smaller surface (weak point). The S_t varies from about 4400 kPa for 0.1% absorption to 2000 kPa for 1.0% absorption, which shows that the asphalt mix tensile strength is affected by segregation. The two groups of specimens can be clearly distinguished. Those that have been sampled in the segregation axis are characterized by an overall absorption greater than 0.5% with lower and more variable S_t, while those that have been sampled outside the axis are characterized by an overall absorption lower than 0.5% with higher S_t.

4.4. Tomodensitometry (CT-scan)

Tomodensitometry (computerized tomography scanning or CT-scan) is an imaging technique that consists of measuring the X-ray absorption by the objects and then by computer processing, of scanning and reconstructing 2D and 3D images of internal structures. As part of these analyses, a series of cores were analyzed by the multidisciplinary laboratory of CT-scan of the Institut national de la recherche scientifique [25].

This technique allows visualization of the distribution of aggregates and air voids within the asphalt cores. Fig. 10 shows that the asphalt layer in the axis propitious to cracking does not necessarily include segregation over the full thickness. In this example, the lower portion of the upper layer (above the interface) comprises many more coarse aggregates and air voids. Air voids reach, in such cases, nearly 20% at specific areas while it can be at most 7% (indicated by a dotted line in the figure) for uniform layers, as prescribed by the MTMDET's requirements. An axis propitious to cracking is characterized by a density gradient due, in part, to the presence of segregation at the base of the layer.

On average, the air voids measured by tomodensitometry are similar to those obtained with conventional tests. However, conventional tests measure air voids over the entire asphalt layer. The difference in voids at the base of the layer is therefore mitigated by the density of the upper part of the core. Moreover, water absorption helps to point out more clearly the presence of a significant network of interconnected voids than the air void measurements in the laboratory. The water absorption results thus corroborate the tomodensitometry results, which indicate the presence of air void concentration zones (more porous areas) at the base of the asphalt layer.

Visualization of the location of the crack within the intact sample is also possible by tomodensitometry thus allowing to better explain the phenomenon. In Fig. 11 (top left), the vertical plane at the center of the core in the direction perpendicular to traffic shows that the crack is present up to a depth of about 6 cm. It is present in the upper part of the core where the air void content is between 5% and 7%. The picture (top right) in the figure shows the path of the crack reaching the interface between the two layers on the periphery of the core. At this location,

Table 1
Test results obtained for each sector investigated.

Sectors		Air void content (%)		Water absorption (%)		Dynamic modulus (MPa)		Tensile strength (kPa)	
		Axis	Off-axis	Axis	Off-axis	Axis	Off-axis	Axis	Off-axis
1	Mean	5.0	4.5	0.9	0.4	7152	7978	2365	4002
	Std deviation	0.6	0.6	0.2	0.0	621	503	659	31
	SDS*	NO		YES		NO		YES	
2	Mean	5.8	5.3	0.8	0.5	5763	6412	2107	3317
	Std deviation	0.3	0.7	0.0	0.1	151	274	852	43
	SDS*	NO		YES		YES		YES	
3	Mean	4.1	2.4	0.9	0.1	5691	7289	2701	4403
	Std deviation	0.2	0.4	0.0	0.0	139	292	232	0
	SDS*	YES		YES		YES		YES	
4	Mean	4.4	4.3	0.5	0.2	6505	6766	3401	4234
	Std deviation	0.4	0.4	0.1	0.0	442	569	316	114
	SDS*	NO		YES		NO		YES	
5	Mean	5.0	4.2	0.6	0.3	6398	7459	3509	4137
	Std deviation	0.2	0.2	0.1	0.0	570	197	294	175
	SDS*	YES		YES		YES		YES	
6	Mean	6.8	5.9	1.1	0.2	6005	8130	2480	3864
	Std deviation	0.0	0.7	0.4	0.2	1001	383	358	415
	SDS*	YES		YES		YES		YES	
7	Mean	6.0	5.0	0.7	0.2	4781	8614	2072	3831
	Std deviation	0.3	0.5	0.1	0.1	494	304	263	375
	SDS*	YES		YES		YES		YES	

* Significantly different statistically.

a failure plane has been created at the interface. Axial sections (bottom figure) identify the location of the crack based on depth.

The sections at 1.5, 3.0, and 4.5 cm depth show that the crack is furrowing between the aggregates even if there is no evidence of high void areas. At a depth of 4.5 cm, the path is only visible in a portion of the core (top section of the axial section), which gives an indication of the level of progress of the crack. On axial sections at 6.0 and 7.5 cm, the crack cannot easily be identified only by one path, but there is the presence of a certain amount of interconnected air voids that represent a dislocation network.

5. Longitudinal thermal cracking phenomenon

Studies have demonstrated that the development of longitudinal cracking, typical of what can be found prematurely on asphalt pavement, is primarily due to downward thermal cracking phenomenon. In the case of new pavement, cracks affecting the surface layer occurred prematurely a few months after works cannot be explained by a concentration of shear stress on surface due to the repeated tire load or by a fatigue effect.

The results of the various tests and analyses of the cases studied confirm that the mechanisms leading to the development of top-down cracking are closely related to the presence of a weakness plane; a clear rectilinear discontinuity affecting the mechanical properties of asphalt. The asphalt in these axes has a particle size distribution and a density different from the rest of the pavement. The decrease in binder content could also be tributary to the difference in particle size distribution, i.e., the existence of a concentration of coarser aggregates which has, for the same volume, a smaller specific surface for bitumen. These axes are characterized by a greater air void concentration. Despite an increase in air void content of only 1 percent, the relationship found with the dynamic modulus and the tensile strength shows that higher void interconnections (indirectly measured by water absorption) have a direct effect on a mix's capacity to distribute stresses and resist cracking.

Since the comparative cores analyzed in the laboratory were not taken directly into the cracks, the segregation is probably more intense or more linearly continuous in the areas that were already cracked. The similarity of voids' distribution found on cracked and uncracked cores gives reason to believe that cracking may extend and develop over time into and toward areas affected by segregation.

The voids measured on all the cores are within the range of values required by the MTMDET, i.e., from 2% to 7%. There is therefore no lack of density due to insufficient compaction. These results also indicate that although the overall increase in air voids in the mix is small, concentrations of air voids could reside and cause a density gradient in the asphalt layer. It is possible that a layer which has a lower density throughout its entire thickness in a problematic axis during laying of mix (thermally detectable) may result in a density gradient created by the effect of com-

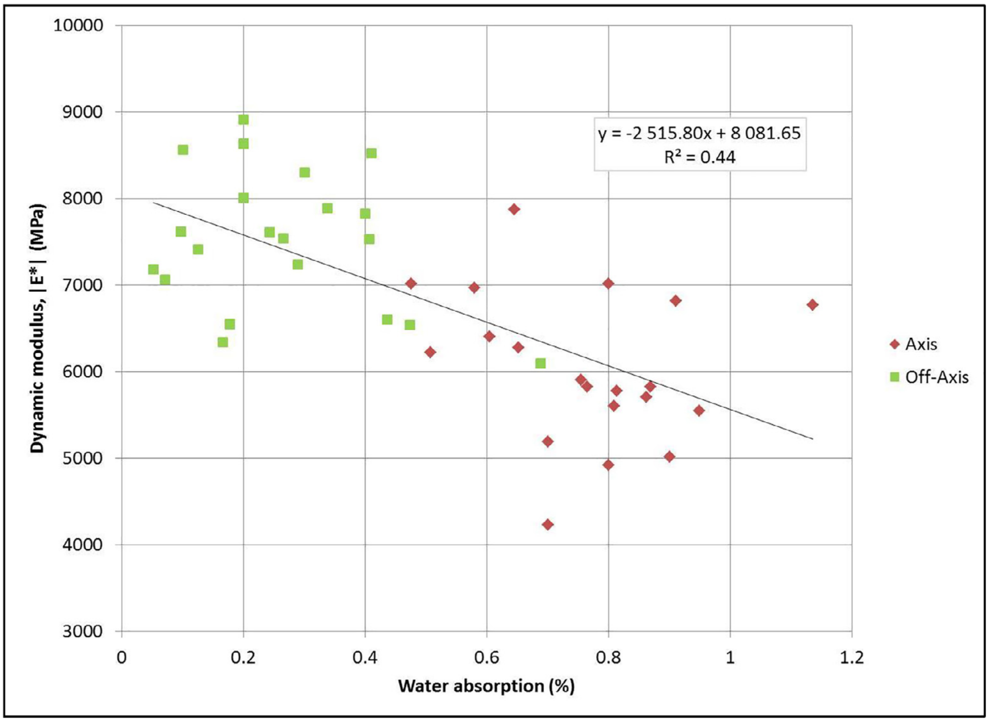

Fig. 8. Relationship between dynamic modulus and water absorption results of the surface layer.

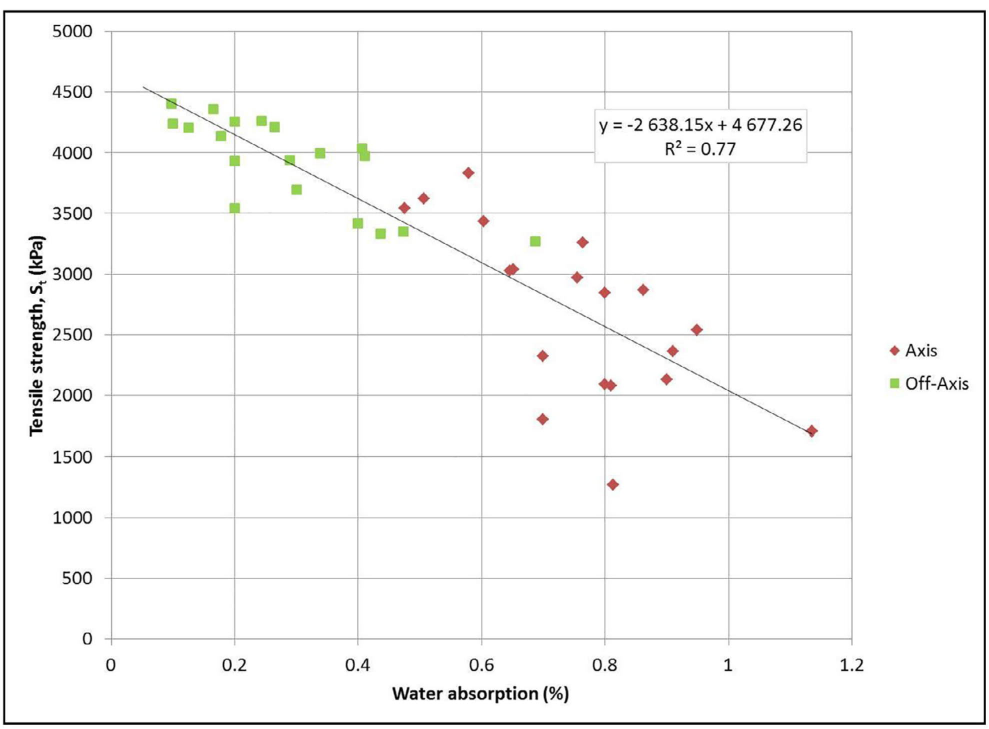

Fig. 9. Relationship between tensile strength and water absorption results of the surface layer.

paction by the surface, thus leaving more voids at the bottom part of that layer.

The distribution of air void concentrations in the asphalt mat, oriented along a line or plane, has an impact on the mechanical properties of the pavement. In addition to having a lower stiffness, the mix in these axes presents less resistance to traction. There is thus possibility of the presence of an area with higher stresses, especially those induced by the thermal contraction forces (acting longitudinally and transversely) characteristics of a northern

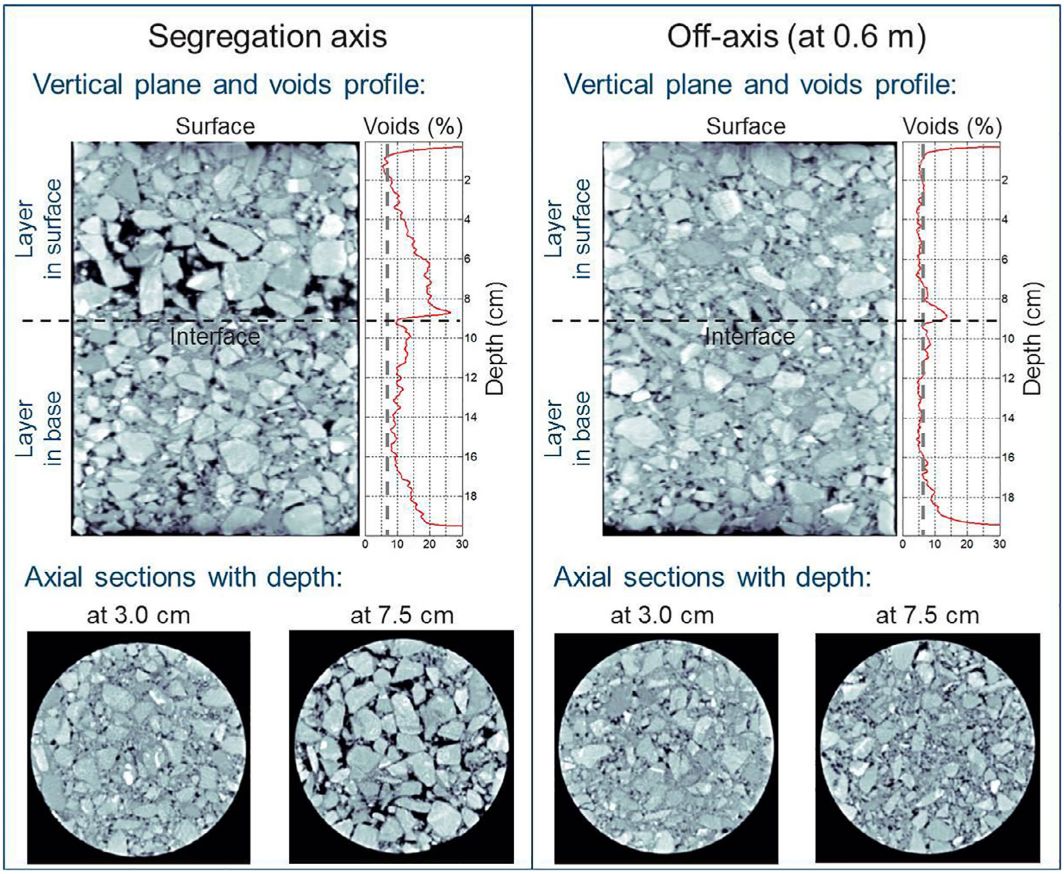

Fig. 10. Tomography results with air void profiles for axis comparison.

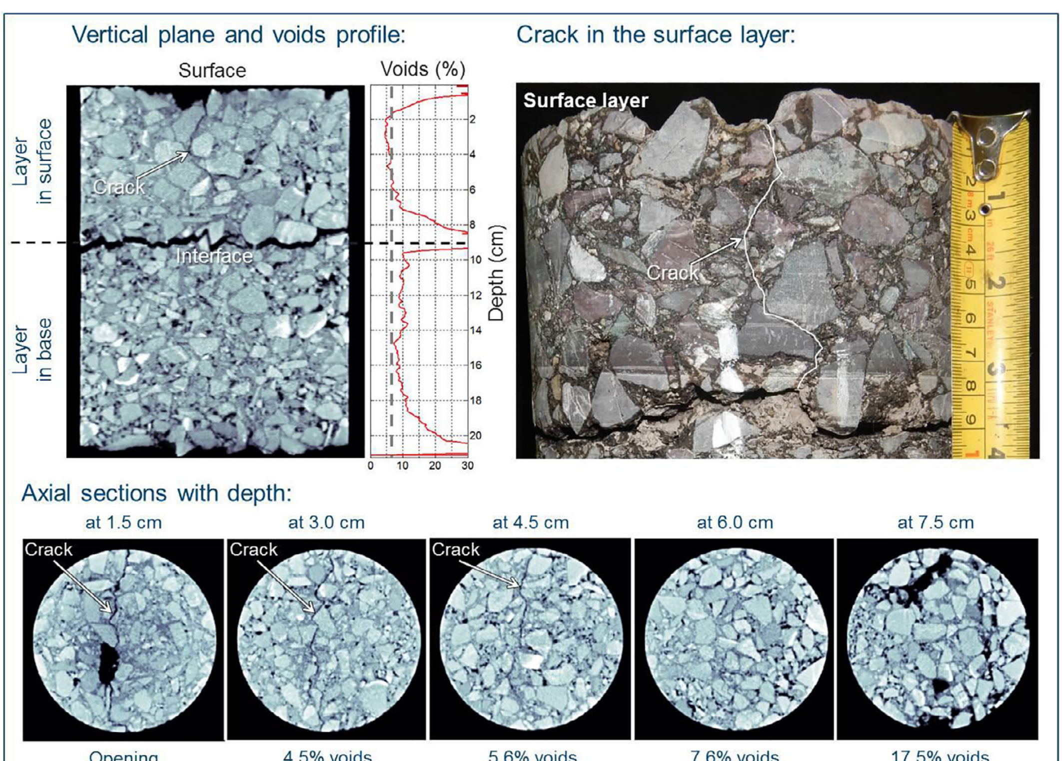

Fig. 11. Tomography results with air void profiles for a core with a crack.

climate. In this situation, the almost continuous plane or planes of weakness on the pavement do not have the ability to evenly well-distribute stresses transversely and this causes the thermal cracking phenomenon longitudinally.

The explanation for the presence of a weakness plane is confirmed by the observations of cores, the results of laboratory analyses, and the results of mechanical tests as well as the CT-scan images.

6. Conclusion

The cases studied indicate that the use of thermography for control purposes is an efficient and reliable approach for detecting thermal streaks in the asphalt mat. The results obtained demonstrate an obvious link between the presence of thermal streaks identified by thermography and the appearance of premature top-down longitudinal cracking.

Conventional laboratory tests confirm that the mix composition may vary slightly locally where cracks develop even if segregation cannot be clearly identified visually. Tomodensitometry and mechanical tests however demonstrate more clearly that in the axis of segregation, porosity (void concentration) in the mix is locally higher which affects its mechanical behavior. The existence of a plane of weakness, physically demonstrated, appears to be the main cause explaining the presence of most longitudinal cracks observed on the Quebec road network. These weakness planes are difficult to detect visually during construction, as well as with conventional measurement methods and analyses.

These studies indicate that the problem of the thermal streak phenomenon is related to defective asphalt placement. The particular thermal signature clearly indicates nevertheless that, over a small width in some specific longitudinal straight axes, the mix is in a different condition during placement in relation to the adjacent asphalt. Although improvements have been made to pavers in recent years, it remains that possible discontinuities can still be detected with infrared.

The use of a quality control procedure on construction site with a disincentive mechanism in case of non-compliance is recommended to incite contractors to make pavers and operations adjustments, make the maintenance of their equipment and perform auto-control to prevent hot mix asphalt poor distribution.

The experience acquired in the application of thermal control and the studies' findings allow an appreciation of the well-founded nature of the method. Thermography proves to be the most appropriate means of control to assess the uniformity of hot mix asphalt's characteristics during paving, making it possible, in particular, to reveal planes of weakness that could cause the development of top-down longitudinal cracking. Also, this method allows evaluation of the effectiveness of the adjustments and improvements made to equipment and work methods related to asphalt paving. It is a recognized practice at the MTMDET, which contributes to the improvement of pavement behavior and durability.

References

[1] M. Lavoie, Using infrared technology for quality control during asphalt placement, in: Proceedings of the 52nd Annual Conference, Canadian Technical Asphalt Association, 2007, pp. 87–111.
[2] Ministère des Transports du Québec (MTQ), Guide de Mesure et d'Identification des Dégradations des Chaussées Souples, Ministère des Transports du Québec, Québec, 2007.
[3] Ministry of Transportation of Ontario (MTO), Manual for Condition Rating of Flexible Pavements – Distress Manifestations, SP-024, Research and Development Branch, Ministry of Transportation of Ontario, Ontario, 1989.
[4] L.A. Myers, R. Roque, B. Birgisson, Propagation mechanisms for surface-initiated longitudinal wheelpath cracks, Transp. Res. Rec. J. Transp. Res. Board 1778 (2001) 113–122, https://doi.org/10.3141/1778-14.
[5] P. Yee, B. Aida, S.A.M. Hesp, P. Marks, K.K. Tam, Analysis of premature low-temperature cracking in three Ontario, Canada, Pavem. Transp. Res. Rec. J. Transp. Res. Board 2006 (1962) 44–51, https://doi.org/10.3141/1962-06.
[6] R.C. Williams, R. Shaidur, Premature Asphalt Concrete Pavement Cracking, Iowa State University, Oregon Department of Transportation and Federal Highway Administration, FHWA-OR-15-16, 2015. http://library.state.or.us/repository/2015/201506181026394/index.pdf.
[7] J.S. Uhlmeyer, K. Willoughby, L.M. Pierce, J.P. Mahoney, Top-down cracking in Washington state asphalt concrete wearing courses, Transp. Res. Rec. J. Transp. Res. Board 1730 (2000) 110–116, https://doi.org/10.3141/1730-13.
[8] T. Svadissant, M. Schorsch, G.Y. Baladi, S. Pinyosunun, Mechanistic analysis of top-down cracks in asphalt pavements, Transp. Res. Rec. J. Transp. Res. Board 2002 (1809) 126–136, https://doi.org/10.3141/1809-15.
[9] T. Pellinen, G. Rowe, Evaluation of Surface (Top Down) Longitudinal Wheel Path Cracking. Joint Transportation Research Program, Final Report FHWA/IN/JTRP-2004/6, Indiana DOT and Purdue University http://docs.lib.purdue.edu/jtrp/93/, 2004.
[10] D. Harmelink, T. Aschenbrener, Extent of top-down Cracking in Colorado, Colorado DOT Research Branch, Report No. CDOT-DTD-R-2003-7, https://www.codot.gov/programs/research/pdfs/2003/topdowncracking.pdf/view, 2003.
[11] T. Aschenbrener, Paver Segregation, Colorado DOT Presentation, North Central Hot Mix Asphalt Technical Workshop and Conference, St. Louis, Missouri, January 12th, 2006.
[12] D. Harmelink, S. Shuler, T. Aschenbrener, Top-down cracking in asphalt pavements: causes, effects, and cures, J. Transp. Eng. Am. Soc. Civil Eng. 134 (1) (2008) 1–6.
[13] Wirtgen, Paver Operations, Presentation, 56th Annual Asphalt Paving Conference, Mt. Pleasant, Michigan, March 20th and 21th 2012. www.apa-mi.org/docs/PaverOperations.pdf.
[14] Washington State Department of Transportation, Infrared Camera Detection of Thermal Differentials Tech Notes, Washington State Department of Transportation, 2000.
[15] M. Lavoie, Expérimentation de la thermographie automatisée au ministère des Transports du Québec, in: Proceedings of the 56th Annual Conference, Canadian Technical Asphalt Association, 2011, pp. 13–26.
[16] American Association of State Highway and Transportation Officials (AASHTO) T322-07 (2011), Standard Method of Test for Determining the Creep Compliance and Strength of Hot-Mix Asphalt (HMA) Using the Indirect Tensile Test Device, Standard Specifications for Transportation and Methods of Sampling and Testing, 2011.
[17] Ministère des Transports du Québec (MTQ), LC 26-690 Fabrication d'éprouvettes cylindriques d'enrobé pour les essais en traction-

compression directe, Recueil des méthodes d'essais LC. Recueil des méthodes d'essais LC, Laboratoire des chaussées, Les Publications du Québec, Canada, 2015. www2.publicationsduquebec.gouv.qc.ca/transports/html/lc4.html.

[18] Ministère des Transports du Québec (MTQ), LC 26-040 Détermination de la densité brute et de la masse volumique des enrobés à chaud compactés, Recueil des méthodes d'essais LC, Laboratoire des chaussées, Les Publications du Québec, Canada, 2015, www2.publicationsduquebec.gouv.qc.ca/transports/html/lc4.html.

[19] Ministère des Transports du Québec (MTQ), LC 26-067 Détermination de la densité et de l'absorption du gros granulat, Recueil des méthodes d'essais LC, Laboratoire des chaussées, Les Publications du Québec, Canada, 2015. www2.publicationsduquebec.gouv.qc.ca/transports/html/lc4.html.

[20] Ministère des Transports du Québec (MTQ), LC 26-700 Détermination du module complexe des enrobés, Recueil des méthodes d'essais LC, Laboratoire des chaussées, Les Publications du Québec, Canada, 2015. www2.publicationsduquebec.gouv.qc.ca/transports/html/lc4.html.

[21] F. Doucet, Dynamic modulus of asphalt mixes in Quebec, in: Proceedings of the 55th Annual Conference, Canadian Technical Asphalt Association, 2010, pp. 331–352.

[22] F. Doucet, M. Laplante-Boivin, B. Auger, Module complexe des enrobés et module réversible des matériaux granulaires pour le dimensionnement mécaniste-empirique des chaussées au Québec, Proceedings of the 100th Annual Conference, Transportation Association of Canada, 2014.

[23] Ministère des Transports du Québec (MTQ), Détermination du module complexe des enrobés, Info DLC, Ouvrages routiers, Vol. 16, No. 4, September 2011. www.transports.gouv.qc.ca/fr/entreprises-partenaires/entreprises-reseaux-routier/info-dlc/Documents/2011/2011-09-info-dlc.pdf.

[24] Ministère des Transports du Québec (MTQ), Module dynamique des enrobés au Québec, Info DLC, Ouvrages routiers, Vol. 17, No. 2, April 2012. www.transports.gouv.qc.ca/fr/entreprises-partenaires/entreprises-reseaux-routier/info-dlc/Documents/2012/2012-04-info-dlc.pdf.

[25] Institut national de recherche scientifique, Multidisciplanary Laboratory of CT-scan. http://ctscan.ete.inrs.ca/en/. 2017 (accessed November 1st 2017).